Long-range magnetic order stabilized by acceptors

Xiaodong Zhang,[1] Jingzhao Zhang,[1] Kinfai Tse,[1] Shengbai Zhang,[2] and Junyi Zhu[1,*]
[1]*Department of Physics, Chinese University of Hong Kong, Hong Kong SAR, China*
[2]*Department of Physics, Applied Physics, and Astronomy, Rensselaer Polytechnic Institute, Troy, New York 12180, USA*

(Received 3 March 2018; revised manuscript received 30 March 2019; published 24 April 2019)

Tuning magnetic order in magnetic semiconductors is a long-sought goal. Here, we propose that a proper mix of acceptors with magnetic dopants may quench local magnetic order in favor of the long-range one. Using Mn and acceptor codoped LiZnAs as an example, we show, by first-principles calculations, the emergence of a long-range magnetic order. This intriguing observation may be understood based on a crossover between an acceptor-free magnetism and a band-coupling magnetism. Our findings pave the way for a precise control of magnetic order in future spintronic devices.

DOI: 10.1103/PhysRevB.99.134435

I. INTRODUCTION

Despite the unique magnetic properties and flexible tunability, which lead to the realization of giant magnetoresistance tunneling device and magnetic memory cell (both based on Mn-doped GaAs [1,2]), the formation of inhomogeneous spin domains is unfavorable for some applications of diluted magnetic semiconductors (DMSs) [3–7]. These domains are formed by an aggregation of magnetic dopants [8–10], as a result of short-range attractions among them [10]. It happens that charge-carrier doping can considerably affect the aggregation of the magnetic dopants. Earlier theory had focused on short-range magnetic interactions as a result of the doping [8,11], for the reason that first-principles calculations at the time were limited by the small cell size and/or an insufficient sampling of the magnetic dopants [12,13]. Experimentally, Kuroda *et al.* also showed that at certain electron-dopant concentrations, the aggregation of Cr in $(Zn_{1-x}Cr_x)Te$ is enhanced [14]. This result can be explained by an energy gain due to an electron-enhanced short-range magnetic attraction among Cr atoms [8].

Long-range magnetic interaction can be mediated by electronic codopants in magnetic semiconductors [4,15–22] or by the van Vleck mechanism [23] or stepping-stone mechanism [24] in carrier-free topological insulators [6,25]. Earlier studies had centered on systems with short-range and long-range mechanisms mixed [11,14]. Whether the short- and long-range interactions between magnetic dopants respond differently to charge-carrier doping remains an open question. To this end, searching for a different paradigm that can suppress all short-range magnetic orders, while simultaneously enhancing long-range orders, would be highly desirable, but unfortunately little has been done along this path both experimentally and theoretically. The reason is simple, as such a path would be against the common consensus that the long-range order is always weaker than the short-range order based on the known fact that the magnetic coupling strength decreases rapidly with the distance between magnetic dopants.

In our view, such a consensus has led to an impasse in advancing the study of DMSs. The consensus is, however, not flawless, as, for example, there is evidence that an acceptor-mediated magnetic order can work against the short-range order which dominates under the acceptor-free condition [8]. In other words, intentionally introduced acceptors could reduce the short-range magnetic coupling strength, thereby mitigating the undesirable aggregation or magnetic phase separation. At the same time, the long-range magnetic order may stay or even be enhanced, as its response to the presence of the acceptors can be qualitatively different from that of the short-range order. We believe such a reasoning raises the hope that with a proper mix of the magnetic dopant and acceptor concentrations, the system can suppress the phases that are in favor of the short-range order by significantly increasing their formation energies.

In this paper, we present theoretical evidence for the rationale and reveal the microscopic mechanisms for the interplay between different magnetic orders in the presence of an acceptor doping. Without the loss of generality (the trend is similar in other I-II-V and II-VI compounds and the results are shown in the Supplemental Material [26]), we consider the magnetic orders in Mn-doped LiZnAs [27], where Li_{Zn} and/or V_{Li} serve as the acceptors. Using density-functional-theory calculations, we uncover a long-range antiferromagnetic (AFM) order, which may be attributed to the fundamental stepping-stone mechanism mediated by the magnetized Zn d and As p states. We also find, in line with the above discussions, that at a proper acceptor concentration, the short-range AFM order can be removed, while the long-range AFM order gives way to a ferromagnetic (FM) order. The net effect is the stabilization of a long-range FM configuration. Our findings thus point to a different direction that may revive the rational design of DMSs.

II. METHODS

All calculations are performed using the projected augmented-wave method [28] and density functional theory within the generalized gradient approximation of

*jyzhu@phy.cuhk.edu.hk

Perdew-Burke-Ernzerhof [29] as implemented in the VASP code [30]. The Mn-doped LiZnAs is simulated by a 2×2×2 supercell (96 atoms). All atoms are relaxed with force tolerance of 0.01 eV/Å. A plane-wave cutoff energy of 500 eV was used in all calculations. For Brillouin-zone integration, a Monkhorst-Pack k-point grid of 4×4×4 was employed. In order to consider the strong correlation effect of transition metals, the local density approximation (LDA)+U method [31] is used. The Hubbard parameter U=3.5 eV and Hund rule exchange parameter J= 0.6 eV are taken, as suggested by Ref. [32]. HSE06 calculations are also performed to check the accuracy of the LDA+U method and it is found that the results of the LDA+U method are qualitatively consistent with the results of HSE calculations. Convergence tests in respect to cell size, energy cutoffs, k points, U, and force cutoffs have been performed.

To simulate the short-range and long-range magnetism, we use a 2×2×2 supercell with two Mn atoms substituting two Zn atoms, which correspond to Mn concentration of 6.25%. Considering the symmetry of LiZnAs, there are five types of inequivalent configurations, corresponding to the first-nearest-neighbor (1st-NN) configuration to fifth-nearest-neighbor (5th-NN) configuration (see the Supplemental Material for details [26]).

The formation energy of Mn-doped LiZnAs is defined as

$$E_f = E(doped) - E(undoped) + n_{Zn}\mu_{Zn} - n_{Mn}\mu_{Mn}, \quad (1)$$

where μ_{Zn} and μ_{Mn} are the chemical potential of Zn and Mn, respectively. And n_{Zn} and n_{Mn} are the number of Zn and Mn, respectively. In the comparison among different magnetic configurations, these two chemical potentials will be canceled.

III. RESULTS AND DISCISSIONS

First, we calculated the relative formation energy without acceptors as a function of different neighboring configurations, as shown in Fig. 1(a). Here, the relative formation energy is calculated in reference to an AFM state of the first-nearest-neighboring (1st-NN) sites, which is the most stable configuration.

Next, we introduced acceptors by replacing Zn atoms with Li atoms. Various Zn sites have been checked and we found that the most stable configuration is obtained by replacing Zn sites that are the nearest neighbors to the magnetic dopants. Still, the total energies are similar for different replacement sites. Also, we calculated the formation energy of the Mn pairs as a function of different doping configurations. To our surprise, the most stable configuration is the FM state with magnetic dopant atoms occupying the fifth-nearest-neighboring (5th-NN) sites and the 1st-NN sites becomes the most unstable [Fig. 1(b)]. This discovery strongly suggests that with the introduction of acceptors, the local magnetic dopants' clustering is largely hindered and the long-range order of magnetic dopants emerges.

This can be further illustrated by the statistically averaged NN distance as a function of the temperature and cell size [Fig. 1(d)]. Without the hole doping, the average Mn-Mn distances at 300 K are 5.43 and 8.05 Å, respectively, for the 2×2×2 and 3×3×3 supercells. Upon hole doping, in both cases the average distances increase, showing

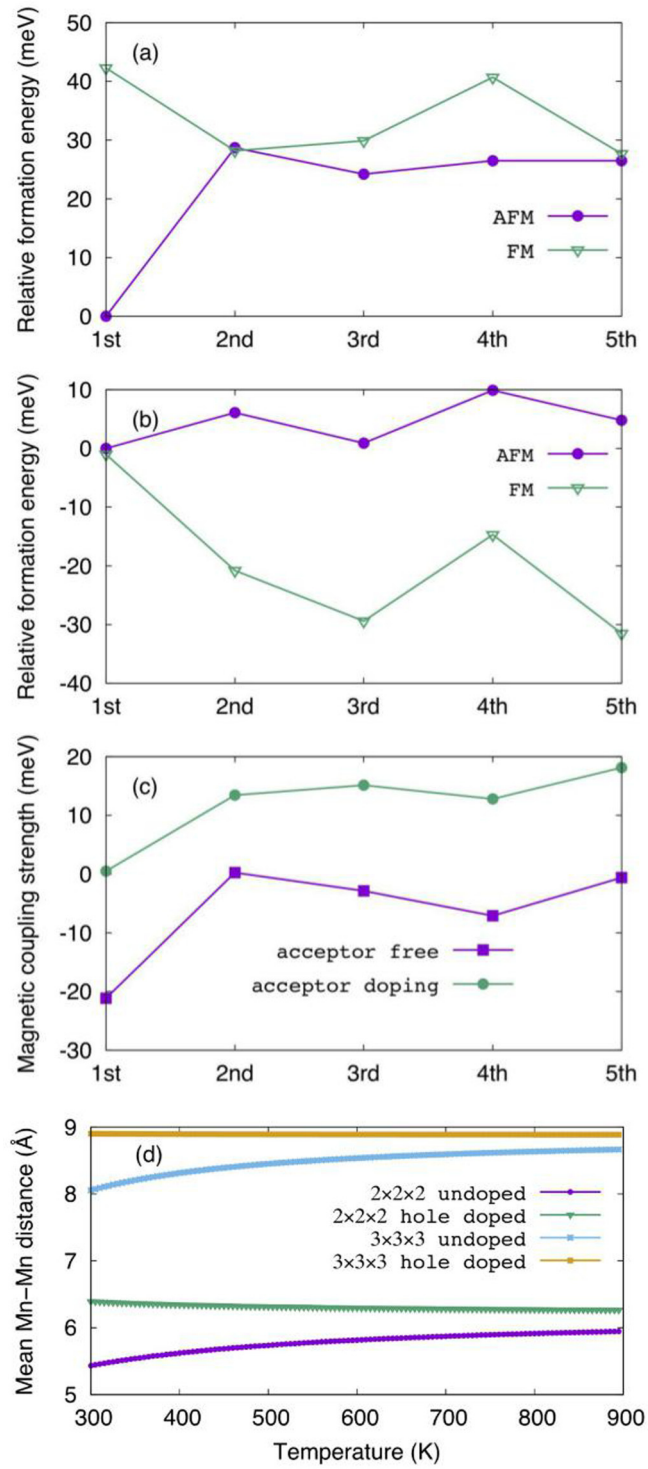

FIG. 1. (a) Relative formation energy of Mn dopants at different nearest-neighboring sites for the acceptor-free case; (b) the energy for the acceptor doping case; (c) magnetic coupling strength of different configurations; (d) average NN distance between a magnetic dopant pair at different cell sizes.

the effectiveness of our strategy. This happens because at the temperature range relevant to experiment, thermal energy is comparable to short-range superexchange interactions. As such, configurational entropy, which is in favor of a

random distribution of the magnetic dopants, competes with the 1st-NN interactions, which is, on the other hand, in favor of the clustering of the dopants. Hole doping breaks this balance against the clustering as it suppresses the superexchange interactions.

To further understand this dramatic change in the relative stabilities of different configurations, we calculated the magnetic coupling strength of each configuration, as shown in Fig. 1(c). The magnetic coupling strength is defined as half of the difference between the AFM and FM states. The calculated results demonstrate that the first-nearest-neighboring sites prefer an AFM state for the acceptor-free case. However, when an acceptor is introduced, the magnetic coupling strength decreases to almost zero. When the distance between the dopant pairs becomes longer, the magnetic order changed from AFM or nonmagnetic to FM. This discovery is different from the "common sense" belief that magnetic coupling strength is the strongest among the neighboring sites and decays very fast when the distance between dopant atoms increases.

In order to understand how acceptor doping changes the magnetic interaction and further influences the relative formation energy, we first need to understand the magnetic interaction in the acceptor-free case.

In the acceptor-free case, the magnetic interaction of the 1st-NN configuration can be explained by the superexchange theory, which suggests that for the half-occupied d state of Mn, the electron hopping from the As p state strongly favors AFM coupling [33–35]. Still, the magnetic coupling between the third- or fourth-nearest neighbors is nonzero. A similar magnetic order has been discovered in the Cr-doped Bi_2Te_3 and Sb_2Te_3 system, where an antibonding state derived from the s lone pair on stepping-stone Bi atoms plays a critical role for the long-range magnetic order. However, in this system, there lacks such an s lone-pair state.

To understand the long-range magnetic coupling mechanism, we calculated the spin texture, as shown in Fig. 2(a). We found that spin density exists near the center of the As and Zn bond, demonstrating a covalent nature. The coupling between the As-p state and Zn-d state is clearly demonstrated in the projected density of states, as shown in Fig. 2(b). The electron hopping among the spin-polarized covalent states near the center of the two As and Zn bonds on the chain lowers the total energy and enhances the long-range correlation between the magnetic dopants.

Further, we substitute the Zn site in the Mn-As-Zn-As-Mn chain by Ca or Cd atoms in order to investigate the role of Zn for such long-range magnetic interaction. We found that the spin density becomes localized around As atoms. This is due to the high ionicity of the Ca and As bonds, as shown in Fig. 2(c). Note that there is no d orbital in Ca^{2+} and the s electron is mostly transferred to the orbitals near the As atom. The electron hopping between the orbitals near different As atoms on the chain is largely hindered because the overlap of orbitals almost disappeared (refer to the Supplemental Material for details [26]). As expected, we found that the magnetic coupling strength is almost zero when Zn sites in the four Mn-As-Zn-As-Mn chains surrounding one Mn atom are substituted by four Ca atoms (Fig. 3). Further, we also substitute four Zn atoms by Cd atoms. We found that the magnetic coupling preserves because the coupling between the d orbitals of Cd and the p orbitals of As is covalent and near the center of the As and Cd bond. Therefore, the electron hopping among these states can lower the total energy and

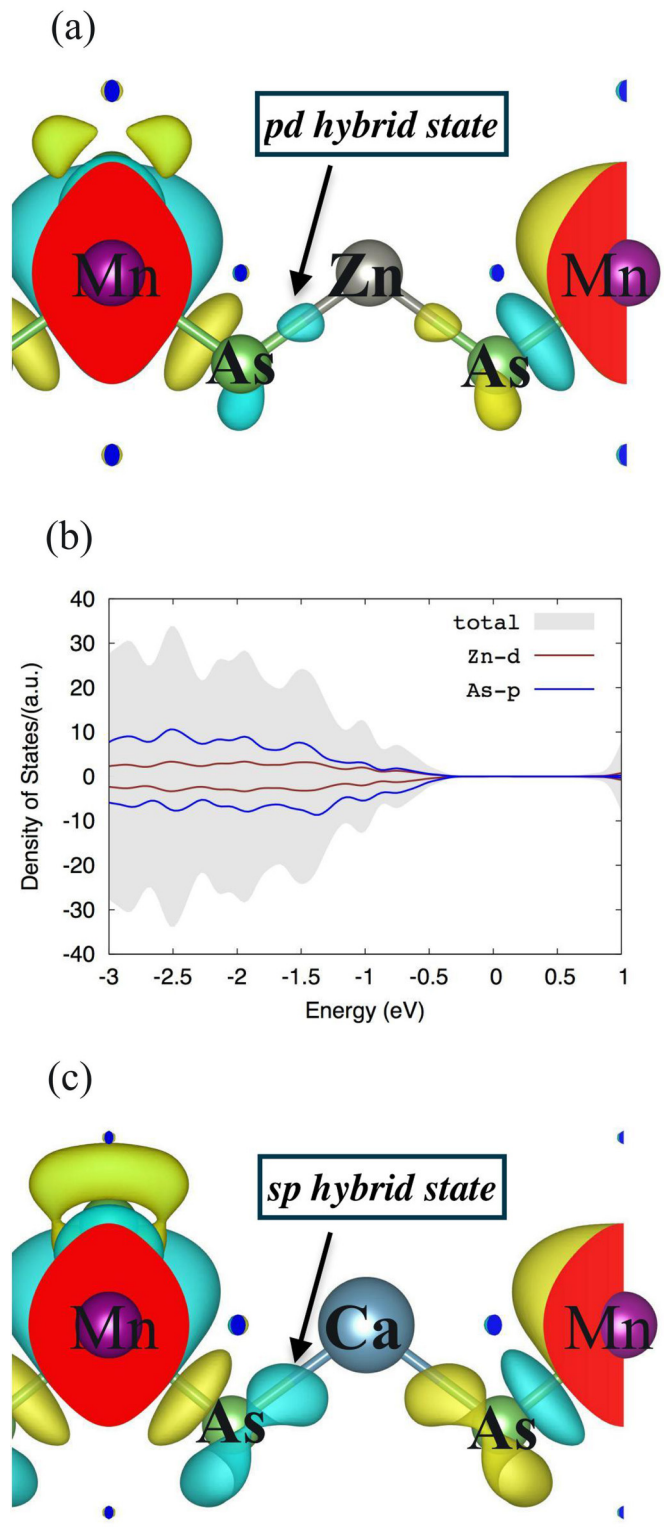

FIG. 2. (a) Local spin density near the dopant in Mn-doped LiZnAs. (b) Projected density of states (PDOS). (c) Local spin density near the dopant in Mn and Ca codoped LiZnAs.

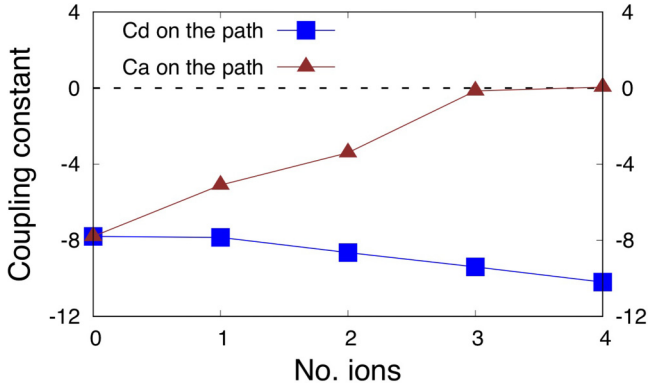

FIG. 3. Changes of the coupling strength with respect to the replaced atoms.

enhance the long-range correlation between Mn dopants. The large coupling strength in the Cd-doping case is due to the enhanced *p-d* coupling strength between Cd and As since the *d* orbital of Cd is higher than that of Zn.

The above analysis demonstrates that the covalent nature of the *p-d* hybridized orbital is the direct reason for such long-range magnetic interactions. *Our results also directly demonstrate that the long-range carrier-free magnetic order mediated by the stepping-stone mechanism can also be extended to p-d hybridized states and to nontopological insulators*.

Next, we will investigate the interplay between acceptor-mediated magnetism and the intrinsic long-range magnetism. We first studied acceptor doping. The band-coupling model [11] suggests that the exchange-coupling strength is sensitive to the position of the *d* level, relative to the valence-band maximum (VBM). Under the crystal field of T_d symmetry, the Mn *d* orbitals are split into lower e_g states and higher t_{2g} states. All five *d* electrons of Mn will occupy these states, which are the majority spin states below the VBM. The minority spin states are all empty and above the VBM. The original band-coupling model [11] proposed that the energy difference between FM and AFM phase is

$$\Delta E_{\mathrm{FM-AFM}} = -\alpha n_h\left(\Delta_{pd}^1 + \Delta_{pd}^2\right) + 6\Delta_{dd}^{1,2}, \qquad (2)$$

where α is a parameter related to the localization of hole (acceptor) states and Mn-Mn distance; n_h is the hole (acceptor) density; the Δ_{pd}^1 and Δ_{pd}^2 are contributions from acceptors and described by Zener's model [15,36,37]; and the $\Delta_{dd}^{1,2}$ is coming from intrinsic magnetic interaction. More details about the band-coupling model and parameters can be found in Ref. [11]. However, this energy difference is not a function of the distance between the dopants. To include the distance as an important variable in the long-range magnetic investigation, we slightly modified the above equation,

$$\begin{aligned}\Delta E_{\mathrm{FM-AFM}} &= -\alpha(R) n_h\left(\Delta_{pd}^1 + \Delta_{pd}^2\right) + 6\beta(R)\Delta_{dd}^{1,2}(n_h) \\ &= n_h J_{\mathrm{acceptors}}(R) + J_{\mathrm{intrinsic}}(R, n_h), \end{aligned} \qquad (3)$$

where R is the distance between the two magnetic atoms; n_h, Δ_{pd}^1, Δ_{pd}^2, and $\Delta_{dd}^{1,2}$ are the same as Eq. (2). $\alpha(R)$ and $\beta(R)$ are magnetic interaction parameters as functions of the distances, based on the acceptor-mediated mechanism and the intrinsic long-range mechanism, respectively. Usually, the decay of $\beta(R)$ is much faster than $\alpha(R)$ because the acceptor state is very delocalized and the interaction range can be very long [38]. The decay of $\beta(R)$ is sensitive to the symmetry of bonding because the intrinsic coupling is mediated by the electron hopping among the magnetized orbitals of the host material. Acceptor-mediated magnetic interaction $J_{\mathrm{acceptor}} = -\alpha(R)(\Delta_{pd}^1 + \Delta_{pd}^2)$ is usually negative, while intrinsic magnetic interaction $J_{\mathrm{intrinsic}} = 6\beta\Delta_{dd}^{1,2}(n_h)$ is usually positive. The $J_{\mathrm{intrinsic}}(R, n_h)$ is not only dependent on distance between the two magnetic atoms, but also influenced by the acceptor density. We further checked the $J_{\mathrm{intrinsic}}$ at different dopant sites and found that the interaction still exists for first-nearest neighbors upon acceptor doping. However, the long-range intrinsic interaction is destroyed by acceptors. This is probably due to the change of electron occupation in the stepping-stone state, which is more sensitive to the acceptor doping than the As-*p* state that mediates the superexchange mechanism. This difference directly leads to the significant different magnetic order upon acceptor incorporation at different magnetic doping sites. A more complete picture can be achieved by strict analysis of many-body effects in the future, which is out of the scope of this paper.

Since the first term in Eq. (3) is dependent upon the acceptor density, it is possible to tune the magnetic coupling by changing the acceptor concentration. If the signs of J_{acceptor} and that of $J_{\mathrm{intrinsic}}$ are opposite, a proper acceptor density will result in zero magnetic interaction for short-range configurations (1st-NN).

In our simulation cell, when we introduce one acceptor by removing one electron from the system, the magnetic coupling becomes almost zero on the first-nearest-neighboring site. When we introduce an Li substitutional defect on a Zn atom that is close to the Mn atom, or when we remove one Li atom that is close to the Mn atom, the magnetism on the nearest-neighboring site configuration also disappears. Therefore, these three calculations confirmed that the acceptor cancels the magnetism on nearest-neighboring configurations.

Further, we checked the magnetic order on other neighboring sites. For the acceptor-free case, the 2nd-NN and the 5th-NN configurations yield almost zero magnetic coupling. Despite the large difference of Mn-Mn distance between 2nd-NN (5.94 Å) and 5th-NN (10.28 Å), the magnetic coupling strengths of 2nd-NN (13.5 meV) and that of 5th-NN (15.1 meV) are similar. These results suggest that acceptor-induced magnetic interaction is almost a constant shift in different neighboring sites, which is different from the fast-decay nature under the acceptor-free condition, as shown in Fig. 1(c). This difference largely cancels the local magnetic interaction and a long-range magnetic interaction emerges. Moreover, the trend is similar even in a $3\times3\times3$ supercell (see part VIII of the Supplemental Material [26]).

Based on all of these calculations and analysis, a strategy on tuning the magnetism of different sites can be proposed. If the short-range magnetic interaction under the acceptor-free condition is different from the acceptor-mediated magnetic interaction, it is possible to incorporate a proper amount of acceptors to largely destroy the short-range magnetism. As a result, the short-range magnetic configuration become unstable and long-range magnetism emerges. Such long-range

magnetic interaction stabilizes long-range configurations and results in a long-range magnetic ordering phase, which can be the global minimum. As shown in Fig. 1(b), the formation energies of the configurations with three or more atoms that separate the dopant atoms (from 2nd-NN to 5th-NN) are all lower than that of the 1st-NN configuration when an acceptor is doped.

In this paper, a sensitive relationship between the stability of short-range vs long-range magnetic order and the concentration of the acceptors is discovered. When a proper amount of codopants is incorporated, the long-range magnetic order can suppress the short-range one and become stable. *Such stability is very important during the growth of DMSs because, once the spinodal decomposition is formed due to the strong short-range magnetic coupling, it is often kinetically forbidden to change the magnetic coupling into long-range ones via postannealing techniques.* These results are also consistent with early experimental discoveries, which suggest that the formation of a nanocrystal (results of spinodal decomposition) can be tuned by acceptors or donors in Cr-doped ZnTe [14]. Therefore, we expect our strategy should be general in various transition metals doped in DMSs and may lead to discoveries of a class of magnetic materials. Our discovery also strongly suggests that it is usually naive to use short-range magnetic order to represent the long-range one. To achieve a complete picture of magnetic order upon different dopant to dopant separations, various doping configurations have to be tested to guarantee the correct results.

IV. SUMMARY

In summary, density-functional-theory calculations reveal that while the long-range AFM order in acceptor-free Mn-doped LiZnAs is mediated by the magnetized *pd* hybridized states, the short-range magnetic order can be largely suppressed by a proper acceptor codoping with Mn. The long-range AFM order also simultaneously ceases as a result of the doping, giving way to a long-range FM order. Realizing such a long-range order is the long-sought goal in the DMS study. Hence, our codoping strategy is expected to impact the study of DMSs broadly, in particular, the explorations of various doped materials with stable long-range ferromagnetism. The acceptor codoping separates the magnetic dopants and can be considered as a strategy to control the magnetic doping sites. A systematic experimental investigation of the proposed codoping strategy is likely to open a different route in materials discovery, as well as new device design principles for tunable spintronic devices.

ACKOWLEDGMENTS

X.Z., J.Z.Z., and J.Y.Z. are grateful for the financial support of the Chinese University of Hong Kong (CUHK) (Grant No. 4053084), University Grants Committee of Hong Kong (Grant No. 24300814), and start-up funding of CUHK. S.B.Z. acknowledges the support by the US Department of Energy Grant No. DESC0002623.

[1] S. Chung, S. Lee, J.-H. Chung, T. Yoo, H. Lee, B. Kirby, X. Liu, and J. K. Furdyna, Phys. Rev. B **82**, 054420 (2010).
[2] S. Mark, P. Dürrenfeld, K. Pappert, L. Ebel, K. Brunner, C. Gould, and L. W. Molenkamp, Phys. Rev. Lett. **106**, 057204 (2011).
[3] H. Ohno, J. Mag. Mag. Mater. **272-276**, 1 (2004).
[4] D. Chiba, M. Sawicki, Y. Nishitani, Y. Nakatani, F. Matsukura, and H. Ohno, Nature (London) **455**, 515 (2008).
[5] S. R. Dunsiger, J. P. Carlo, T. Goko, G. Nieuwenhuys, T. Prokscha, A. Suter, E. Morenzoni, D. Chiba, Y. Nishitani, T. Tanikawa, F. Matsukura, H. Ohno, J. Ohe, S. Maekawa, and Y. J. Uemura, Nat. Mater. **9**, 299 (2010).
[6] C.-Z. Chang, J. Zhang, X. Feng, J. Shen, Z. Zhang, M. Guo, K. Li, Y. Ou, P. Wei, L.-L. Wang, Z.-Q. Ji, Y. Feng, S. Ji, X. Chen, J. Jia, X. Dai, Z. Fang, S.-C. Zhang, K. He, Y. Wang, L. Lu, X.-C. Ma, and Q.-K. Xue, Science **340**, 167 (2013).
[7] C. Z. Chang, P. Tang, Y. L. Wang, X. Feng, K. Li, Z. Zhang, Y. Wang, L. L. Wang, X. Chen, C. Liu, W. Duan, K. He, X. C. Ma, and Q. K. Xue, Phys. Rev. Lett. **112**, 056801 (2014).
[8] J. L. F. Da Silva, G. M. Dalpian, and S. H. Wei, New J. Phys. **10** (2008).
[9] P. Němec, V. Novák, N. Tesařová, E. Rozkotová, H. Reichlová, D. Butkovičová, F. Trojánek, K. Olejník, P. Malý, R. P. Campion, B. L. Gallagher, J. Sinova, and T. Jungwirth, Nat. Commun. **4**, 1422 (2013).
[10] T. Dietl, K. Sato, T. Fukushima, A. Bonanni, M. Jamet, A. Barski, S. Kuroda, M. Tanaka, P. N. Hai, and H. Katayama-Yoshida, Rev. Mod. Phys. **87**, 1311 (2015).
[11] G. M. Dalpian and S.-H. Wei, Phys. Status Solidi B **243**, 2170 (2006).
[12] B. Deng, Y. Zhang, S. B. Zhang, Y. Wang, K. He, and J. Zhu, Phys. Rev. B **94**, 054113 (2016).
[13] B. Deng, F. Liu, and J. Zhu, Phys. Rev. B **96**, 174404 (2017).
[14] S. Kuroda, N. Nishizawa, K. Takita, M. Mitome, Y. Bando, K. Osuch, and T. Dietl, Nat. Mater. **6**, 440 (2007).
[15] T. Dietl, H. Ohno, F. Matsukura, J. Cibert, and D. Ferrand, Science **287**, 1019 (2000).
[16] H. Ohno, D. Chiba, F. Matsukura, T. Omiya, E. Abe, T. Dietl, Y. Ohno, and K. Ohtani, Nature (London) **408**, 944 (2000).
[17] T. Dietl, H. Ohno, and F. Matsukura, Phys. Rev. B **63**, 195205 (2001).
[18] D. Chiba, M. Yamanouchi, F. Matsukura, and H. Ohno, Science **301**, 943 (2003).
[19] F. Matsukura, Y. Tokura, and H. Ohno, Nat. Nanotech. **10**, 209 (2015).
[20] Y. Deng, Y. Yu, Y. Song, J. Zhang, N. Z. Wang, Z. Sun, Y. Yi, Y. Z. Wu, S. Wu, J. Zhu, J. Wang, X. H. Chen, and Y. Zhang, Nature **563**, 94 (2018).
[21] N. Lu, P. Zhang, Q. Zhang, R. Qiao, Q. He, H.-B. Li, Y. Wang, J. Guo, D. Zhang, Z. Duan, Z. Li, M. Wang, S. Yang, M. Yan, E. Arenholz, S. Zhou, W. Yang, L. Gu, C.-W. Nan, J. Wu, Y. Tokura, and P. Yu, Nature (London) **546**, 124 (2017).

[22] S.-C. Tsang, J. Zhang, K. Tse, and J. Zhu, Phys. Rev. Mater. **3**, 024603 (2019).
[23] R. Yu, W. Zhang, H.-J. Zhang, S.-C. Zhang, X. Dai, and Z. Fang, Science **329**, 61 (2010).
[24] C. Chan, X. Zhang, Y. Zhang, K. Tse, D. Bei, J. Zhang, and J. Zhu, Chin. Phys. Lett. **35**, 017502 (2018).
[25] C.-Z. Chang, W. Zhao, D. Y. Kim, H. Zhang, B. A. Assaf, D. Heiman, S.-C. Zhang, C. Liu, M. H. W. Chan, and J. S. Moodera, Nat. Mater. **14**, 473 (2015).
[26] See Supplemental Material at http://link.aps.org/supplemental/10.1103/PhysRevB.99.134435 for details of the results and analyses.
[27] Z. Deng, C. Q. Jin, Q. Q. Liu, X. C. Wang, J. L. Zhu, S. M. Feng, L. C. Chen, R. C. Yu, C. Arguello, T. Goko, F. Ning, J. Zhang, Y. Wang, A. A. Aczel, T. Munsie, T. J. Williams, G. M. Luke, T. Kakeshita, S. Uchida, W. Higemoto, T. U. Ito, B. Gu, S. Maekawa, G. D. Morris, and Y. J. Uemura, Nat. Commun. **2**, 422 (2011).
[28] P. E. Blöchl, Phys. Rev. B **50**, 17953 (1994).
[29] J. P. Perdew, A. Ruzsinszky, G. I. Csonka, O. A. Vydrov, G. E. Scuseria, L. A. Constantin, X. Zhou, and K. Burke, Phys. Rev. Lett. **100**, 136406 (2008).
[30] G. Kresse and J. Furthmüller, Phys. Rev. B **54**, 11169 (1996).
[31] S. L. Dudarev, G. A. Botton, S. Y. Savrasov, C. J. Humphreys, and A. P. Sutton, Phys. Rev. B **57**, 1505 (1998).
[32] J. Mašek, J. Kudrnovský, F. Máca, B. L. Gallagher, R. P. Campion, D. H. Gregory, and T. Jungwirth, Phys. Rev. Lett. **98**, 067202 (2007).
[33] P. W. Anderson, Phys. Rev. **79**, 350 (1950).
[34] J. B. Goodenough, Phys. Rev. **100**, 564 (1955).
[35] K. Junjiro, J. Phys. Chem. Solids **10**, 87 (1959).
[36] C. Zener, Phys. Rev. **81**, 440 (1951).
[37] T. Dietl, A. Haury, and Y. Merle d'Aubigné, Phys. Rev. B **55**, R3347 (1997).
[38] *Fundamentals of Semiconductors–Physics and Materials Properties*, edited by P. Yu and M. Cardona (Springer-Verlag, Berlin, 2010).